Repulsive Interactions Induced by Specific Adsorption: Anomalous Step Diffusivity and Inadequacy of Nearest-Neighbor Ising Model (Part II Theory)

Harald Ibach[1] and Margret Giesen[2*]

Mohammad Al-Shakran, Ludwig A. Kibler, Timo Jacob[3]

[1]*Peter Grünberg Institute (PGI-3), Jülich Forschungszentrum GmbH, 52425 Jülich, Germany.*

[2]*Peter Grünberg Institute (PGI-6), Jülich Forschungszentrum GmbH, 52425 Jülich, Germany.*

[3]*Institut für Elektrochemie, Universität Ulm, Albert-Einstein-Allee 47, 89069 Ulm, Germany.*

Keywords: nearest-neighbor Ising model; next-nearest-neighbor Ising model; repulsive interactions; step diffusivity; step line tension; specific adsorption

Abstract:

This is *Part II* of two closely related papers, where we show that the strong repulsive interaction caused by specifically adsorbed anions leads to a failure of the nearest-neighbor Ising model to describe structures on electrode surfaces. In this part, an analytical form of the step diffusivity is derived in terms of nearest and next-nearest neighbor interactions for steps with a mean direction along ⟨110⟩ (the close-packed direction). With the help of a further analytical expression for the diffusivity of steps with ⟨100⟩ mean orientation a simple scheme is developed whereby the nearest and next-nearest interaction energies can be extracted from the experimental values for the diffusivity along the ⟨110⟩ - and ⟨100⟩-directions. The method is applicable to repulsive and attractive next-nearest neighbor interactions, both for surfaces in vacuum and in contact with an electrolyte. An example is presented in *Part I*, where we apply our approach to Au(100) in Br^--, Cl^-- and SO_4^{2-}containing electrolytes.

* **Corresponding author.** Email: m.giesen@fz-juelich.de;

http://www.fz-juelich.de/SharedDocs/Personen/PGI/PGI-6/EN/Giesen_M.html?nn=545850

1. Introduction

The statistical analysis of step fluctuations and island perimeter fluctuations is one of the few windows which enables a view onto the energetics of atoms and atomic motions at the solid-electrolyte interface. This window is particularly precious as it allows the study of exactly those processes which are active at ambient temperature and therefore important in all practical application of electrochemistry. One may even argue that the view provided by statistical methods has even a certain element of uniqueness, since the view focuses on the rate determining steps in transport processes and on the energetics of those structures which are not frozen-in at ambient temperature. The statistical analysis of step and island perimeter fluctuations has therefore a considerable tradition especially in application to single crystal electrode surfaces [1-7].

The theoretical analyses of earlier results concerning equilibrium fluctuations and transport processes on electrode surfaces took merely nearest-neighbor interactions between atoms into account. Kinks within a step e.g., were assumed to possess the energy proportional to their length [1, 8, 9], an assumption equivalent to allow for nearest-neighbor (NN) interactions only (see Sect. 2). In particular on (100) surfaces where the in-plane coordination is only four, next-nearest-neighbor (NNN) interactions need be taken into account. For Cu(100) surfaces in vacuum, e.g., attractive NNN interaction energies of 1/4 of the NN interaction energies need to be invoked to describe the step diffusivity as a function of step-orientation [10].

Addition of NNN interactions has consequences for the entire functional dependence of the diffusivity on the angle of orientation. This dependence is described by a set of interwoven, complex equations which have to be solved together [11, 12]. To match those

to experimental curves for a particular set of energies is a rather arduous task. Fortunately, there is a much easier path.

This paper shows that NN and NNN interactions on fcc (100) surfaces can be extracted just from two values of the diffusivity, i.e., the diffusivity of steps oriented along $\langle 110 \rangle$ (i.e. $\theta = 0°$) and $\langle 100 \rangle$ (i.e. $\theta = 45°$). At $\theta = 45°$, the diffusivity is almost entirely due to geometrically forced kinks [13]. The diffusivity caused by those is described by a simple equation, even for the entire angle range. Specifically at $\theta = 45°$ the diffusivity depends solely on the NNN interaction, so that the NNN interaction can be calculated directly from the diffusivity. At $\theta = 0°$, geometrically forced kinks do not exist and the diffusivity is entirely caused by thermally excited kinks. The diffusivity is then a simple function of the energy of kinks as function of their length. These energies are conveniently expressed in terms of NN and NNN interactions. Thus the two parameters for NN and NNN interaction energies can be extracted just from two data points on the diffusivity vs. angle curve.

We remark that the statistical mechanics of steps is equivalent to that of a phase separation line within the Ising model for a two-dimensional antiferromagnetic lattice and has been treated in this context by many authors (see e.g. [14-16]). There is furthermore ample literature on the statistical mechanics of interfaces and 2D equilibrium shapes (see e. g. [17]). These papers; however, do not explicitly discuss the experimental quantity of interest here, which is the diffusivity of steps. They furthermore display great deal of abstractness. It is therefore felt that a simple derivation of the relevant equations in the context of our experimental analysis is in order.

Part II is organized as follows. The next section considers the contribution of NN and NNN interactions on the energy of kinks of variable length. It is shown that the resulting expressions for the kink energy can be mapped onto the model in which the kink energy is

split into a contribution of a corner-energy and an energy proportional to the length of the kink. The closed expression for the diffusivity is easily derived for that case. Section 3 considers the diffusivity due to geometrically forced kinks. Section 4 shows that the line tension of ⟨110⟩ oriented steps can be expressed in terms of the same energy parameters for the NN and NNN interaction.

2. Thermally excited kinks in presence of next-nearest neighbor interactions

The considerations to follow are based on the ***T**errace **S**tep **K**ink* (TSK) model of surfaces which assumes that the surface consists of flat terraces separated by steps in such a way that an unequivocal numbering of the steps by an index *i* is possible [18]. The steps are allowed to have kinks, but no overhangs so that the position of a step is uniquely described by a single Cartesian $y_i(x)$ for each step *i*.

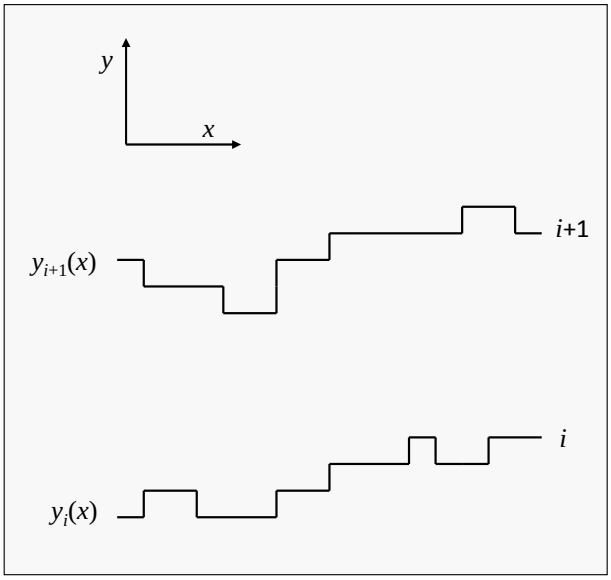

Fig. 1: Top view onto two steps to illustrate the definition of the coordinates. In the TSK-model overhangs are not permitted so that $y_i(x)$ uniquely defines a position on a step.

Fig. 1 shows a top view on step positions on a surface with square symmetry (e.g. ⟨110⟩ steps on $\{100\}$ surfaces of an fcc-material). The defining equation for the diffusivity of step *i* is [19-21]

$$\left\langle \left(y_i(x) - y_i(x_0)^2\right)\right\rangle / a_\perp^2 = (b^2 / a_\perp^2)\left|x - x_0\right| / a_\parallel \qquad (1)$$

when the coordinate *x* is along the ⟨110⟩ direction of the step and *y* the coordinate perpendicular to it. The symbols $a_\parallel$ and $a_\perp$ stand for the atom length unit parallel and perpendicular to the ⟨110⟩ direction, respectively ($a_\parallel = a_\perp$ for fcc (100) surfaces). We note that eq. (1) is the TSK analog of the continuum equation for a freely meandering step

$$\langle \left(y_i(x) - y_i(x_0)\right)^2 \rangle = \frac{k_B T}{\tilde{\beta}(\theta)} |x - x_0| \qquad (2)$$

in which $\tilde{\beta}$ is the stiffness of the step. Within the TSK-model the step meanders because of the presence of kinks of discrete length in units of $a_\perp$. The diffusivity of a step is then given by the normalized sum over the Boltzmann probabilities to have kinks with length of *n*-atomic distances $a_\perp$

$$\frac{b^2}{a_\perp^2} \equiv \langle n^2 \rangle = 2 \frac{\sum_{n=1}^{\infty} n^2 e^{-\frac{\varepsilon_k(n)}{k_B T}}}{1 + 2\sum_{n=1}^{\infty} e^{-\frac{\varepsilon_k(n)}{k_B T}}}. \qquad (3)$$

Here $\varepsilon_k(n)$ is the energy required to create a kink with a length of $na_\perp$. The factor 2 before the sums takes into account that kinks can have two different orientations.

NNN interactions have a nontrivial effect on the energy of kinks as function of their length. This is illustrated with Fig. 2. Extracting a pair of atoms from a step edge and placing

them onto a straight step creates four kinks of single atom length. As illustrated in Fig. 2(a) by solid bars, four NN bonds are broken in the process; however, two of them are regained. Broken NNN bonds are completely regained. Hence, NNN interactions do not contribute to the creation energy of a single atom length kink. The energy per kink for a single atom kink is therefore half the energy required to break a single nearest-neighbor bond. We denote this energy as ϵ_{NN} so that $\varepsilon_{\mathrm{k}}(n=1)=\epsilon_{\mathrm{NN}}$. We remark that the energy for this special case is often noted in literature simply as $\varepsilon_{\mathrm{k}} \equiv \varepsilon_{\mathrm{k}}(n=1)$.

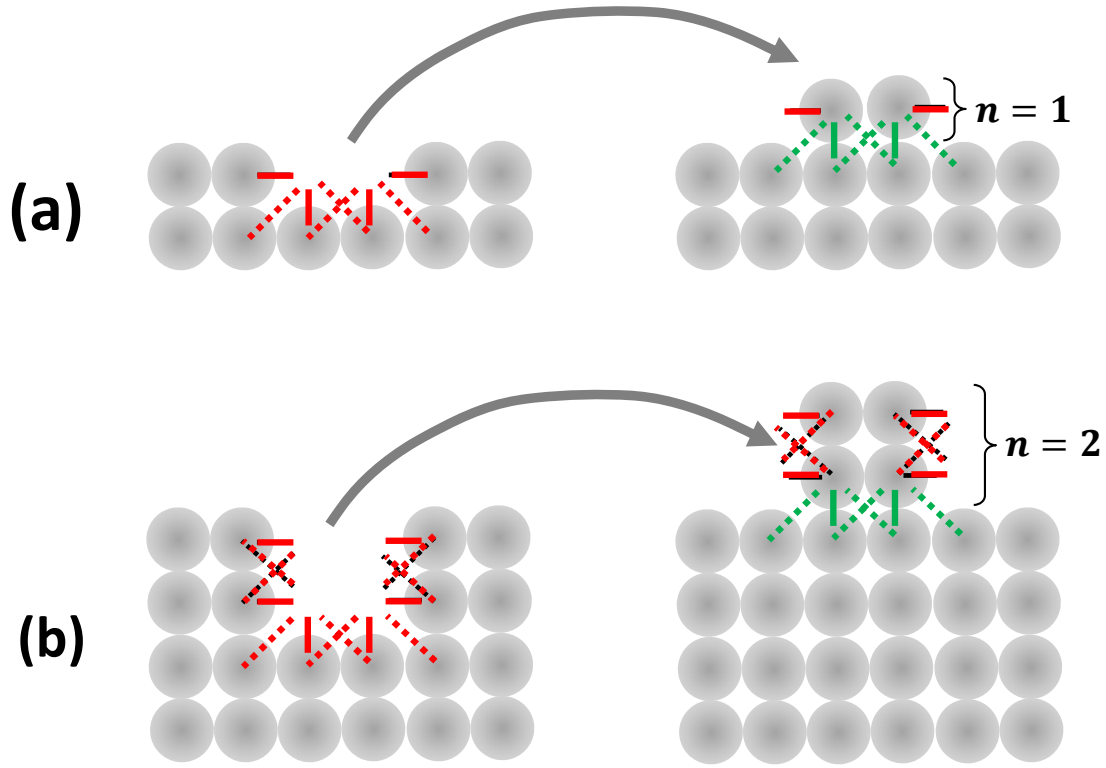

Fig. 2: Solid and dashed lines mark broken NN and NNN bonds, respectively. (a) Extracting two atoms from a step edge and placing them onto the step creates four kinks of single atom length. Four NN bonds are broken in the process (red), two of them regained (green). Broken NNN bonds are completely regained. Hence, the energy per single-atom kink ($n=1$) is $\varepsilon_{\mathrm{k}}(1)=\epsilon_{\mathrm{NN}}$ where ϵ_{NN} denotes half the energy to break a single NN bond. (b) The creation of a kink of two atoms length ($n=2$) requires the net breaking four NN and four NNN bonds . The creation energy per kink is $\varepsilon_{\mathrm{k}}(2)=2\epsilon_{\mathrm{NN}}+2\epsilon_{\mathrm{NNN}}$.

The creation of kinks with more than a single atom length $a_\perp$ however, does involve the breaking of NNN bonds. This is illustrated by Fig. 2(b) for the case of two atom long kinks (n=2). We consider first the nearest neighbor bonds. Six of them are broken in the process, two of them regained. Hence, the creation of two-atom long kinks requires to break four NNN bonds, hence the energy $2\epsilon_{\mathrm{NN}}$, twice as much as a kink of single atom length.

In terms of NNN bonds eight are broken; however, four of them regained. Hence, one NNN bond is broken per kink to which we assign the energy $2\epsilon_{\mathrm{NNN}}$ (i.e. $\epsilon_{\mathrm{NNN}}$is half the energy to break a NNN bond). The total creation energy per kink of n=2 length is therefore $\varepsilon_{\mathrm{k}}(2) = 2\epsilon_{\mathrm{NN}} + 2\epsilon_{\mathrm{NNN}}$.

For each additional atom length two more of the NNN energies are to be added. In general we therefore have

$$\varepsilon_{\mathrm{k}}(n) = n\epsilon_{\mathrm{NN}} + 2(n-1)\epsilon_{\mathrm{NNN}} = n(\epsilon_{\mathrm{NN}} + 2\epsilon_{\mathrm{NNN}}) - 2\epsilon_{\mathrm{NNN}}. \quad (4)$$

We note that this equation is equivalent to eq. 2 in [14] derived in the context of the 2D Ising lattice. The energy for $\varepsilon_{\mathrm{k}}(n)$ therefore consists of two parts, an energy proportional to the kink length

$$n\varepsilon_1 = n(\epsilon_{\mathrm{NN}} + 2\epsilon_{\mathrm{NNN}}) \quad (5)$$

and a "corner energy" [22]

$$\varepsilon_c = -2\epsilon_{\mathrm{NNN}}. \quad (6)$$

Note that the "corner energy" is negative for positive ϵ_{NNN} i.e. attractive NNN interactions and vice versa. With the ansatz for the length dependence of the kink energies, the sums in eq. (3) are executed to yield

$$b^2 / a_\perp^2 \equiv \left\langle n^2 \right\rangle = \frac{2cq(1+q)}{(1-q)^2(1-q+2cq)} \quad \text{with} \quad c = \mathrm{e}^{-\frac{\varepsilon_{\mathrm{c}}}{k_{\mathrm{B}}T}} \text{ and } \quad q = \mathrm{e}^{-\frac{\varepsilon_1}{k_{\mathrm{B}}T}} . \qquad (7)$$

(Eq. (7) was derived previously in [23] as eq. (5.26). However, there the last term in the denominator erroneously reads $2cq^2$ instead of $2cq$). As was brought to our attention by T.L. Einstein, our eq. (7) also corrects the corresponding expression in table 1 of ref. [24].

For a better understanding of the role of NNN interactions for the microscopic structure of steps, it is useful to compare the meandering of $\langle 110 \rangle$ steps with and without repulsive NNN interactions. For that purpose we plot out steps using the probability to find a kink of length n

$$w(n) = 2\frac{e^{-\frac{\varepsilon_k(n)}{k_B T}}}{1+2\sum_{n=1}^{\infty} e^{-\frac{\varepsilon_k(n)}{k_B T}}} \quad , \qquad (8)$$

The parameters in $\varepsilon_{\mathrm{k}}(n)$, namely ϵ_{NN} and ϵ_{NNN}, are taken from two experimental examples. One is for the SO_4^{-2} electrolyte at the potential *E* = +0.3 V SCE for which $\epsilon_{\mathrm{NN}} = 43\ \mathrm{meV},\ \epsilon = 0\ \mathrm{meV}$ (Table 3 of Part I). The other is for the Br^- containing electrolyte at *E* = +0.17 V SCE for which $\epsilon_{\mathrm{NN}} = 98\ \mathrm{meV}, \epsilon_{\mathrm{NNN}} = -42\ \mathrm{meV}$ was found (Table 1 of part I). These examples were chosen since for these parameters steps have about the same diffusivity. Due to the different NNN interactions, the microscopic structure is qualitatively different (Fig. 3). The

red line depicts the step for the SO_4^{2-} electrolyte with no NNN interactions. The orange line is representative for the Br^- containing electrolyte with strong repulsive NNN interaction. Obviously, the appearance of the two steps is qualitatively different, despite the fact that they have about the same diffusivity. In the case of strong repulsive interactions (the Br^- containing electrolyte), kinks are longer on the average length; however, they are also much rarer.

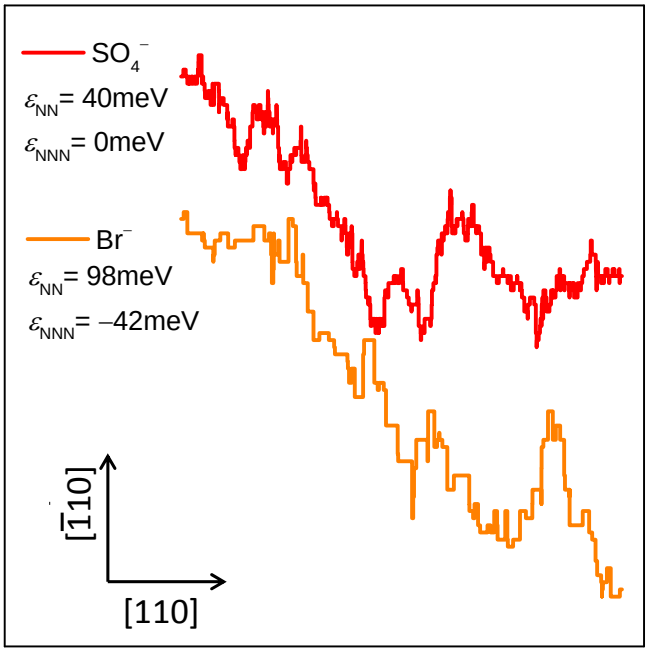

Fig. 3: Profiles for freely meandering, $[110]$ oriented steps. The horizontal scale encompasses 10^4 atom lengths. The vertical axis is enlarged by a factor 160. The steps are not fixed in average orientations, so that they deviate from the $\langle 110\rangle$ direction by the angle $\theta = arc\tan(\sqrt{\langle n^2\rangle})$. The orange line is representative for the Br^- containing electrolyte ($\epsilon_{NN} = 98$ meV, $\epsilon_{NNN} = -42$ meV), the red line for the SO_4^{2-}-electrolyte ($\epsilon_{NN} = 43$ meV, $\epsilon_{NNN} = 0$ meV). Both steps have about the same diffusivity; however, kinks are rarer and longer in the Br^- containing electrolyte.

The reason for the different microscopic structure of the steps becomes clear when one takes a look at the energy of kinks as function of the length on the one hand and the contribution of those kinks of length *n* to the diffusivity

$$\frac{b^2(n)}{a_\perp^2} = 2\frac{n^2 e^{-\frac{\varepsilon_k(n)}{k_B T}}}{1+2\sum_{n=1}^{\infty} e^{-\frac{\varepsilon_k(n)}{k_B T}}} \qquad (9)$$

In Fig. 4, $w(n)$ (eq. (8)) and $b^2(n)/a_\perp^2$ (eq. (9)) are plotted as circles and squares, respectively. The solid orange symbols stand for a case of strong repulsive NNN interactions, as realized with Br^- containing electrolytes. The open red symbols stand for the case of zero NNN interactions, as realized in the SO_4^{2-} containing electrolyte. In that latter case, $w(n)$ is large for small n; however, falls off more rapidly than in the Br^- case. The diffusivity is mainly due to one and two atom long kinks (see red open squares in Fig. 4).

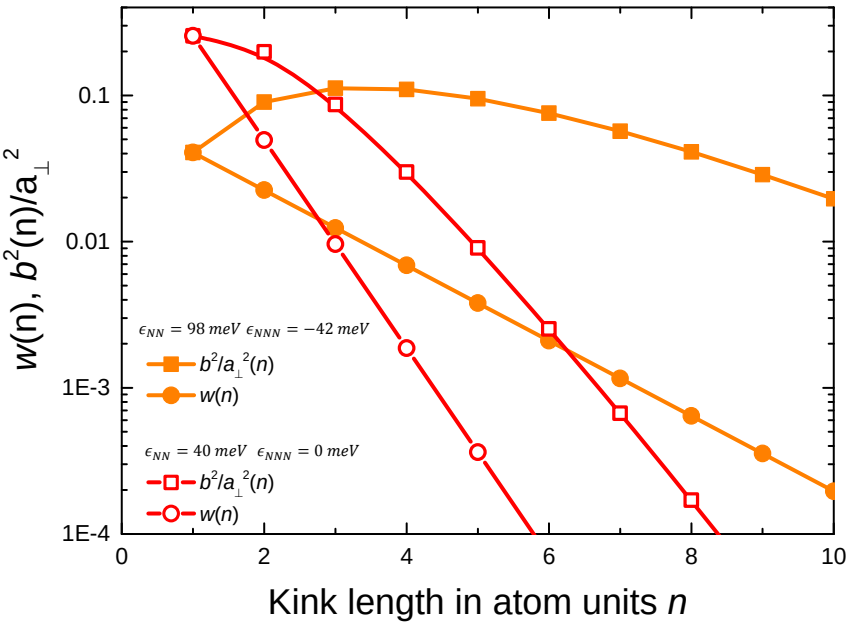

Fig. 4: The probability $w(n)$ to find a kink of length n and the contribution to the diffusivity $b^2(n)/a_\perp^2$ made by kinks of length *n* is plotted as circles and squares, respectively. The solid orange and open red symbols stand for a case of strong (Br^-) and zero (SO_4^{2-}) repulsive NNN interactions, respectively.

For the Br^- case with strong repulsive NNN interaction, the energy required to create a single kink is $\epsilon_{\mathrm{NN}} = 98\,\mathrm{meV}$, the energy required to create a kink of length $2a_\perp$ however, is only

marginally higher ($\varepsilon_{\mathrm{k}}(2) = 2 \cdot 98\ \mathrm{meV} - 2 \cdot 42\ \mathrm{meV} = 110\ \mathrm{meV}$). Since the contribution of kinks to the diffusivity is proportional to n^2, kinks of length $2a_\perp$ contribute more to the diffusivity than kinks of length $1a_\perp$ (see solid orange squares in Fig. 4). Even kinks of length up to $n = 7$ make a larger contribution to the diffusivity than kinks of length $1a_\perp$, despite the fact that they are rare.

3. Geometrically forced kinks

Steps deviating from the $\langle 110 \rangle$ orientation by an angle θ must have a certain fraction of kinks of a sign dictated by the angle θ. The positions of these kinks are randomly distributed, which gives those steps non-zero diffusivity, even at zero temperature. These kinks are called "*geometrically forced*" kinks. Within the NNN model, the diffusivity caused by forced kinks is given by a simple expression [10]:

$$\frac{b^2(\theta)}{a_\perp^2} = \frac{\sin(2\theta)}{2}\sqrt{1 - [1 - 2\exp(-2\,\epsilon_{\mathrm{NNN}}/k_{\mathrm{B}}T)]\,\sin(2\theta)} \qquad (10)$$

The diffusivity due to forced kinks vanishes for $\theta = 0°$, as it must be. In the absence of NNN interactions ($\epsilon_{\mathrm{NNN}} = 0$), the diffusivity due to forced kinks is simply

$$\frac{b^2(\theta)}{a_\perp^2} = \frac{\sin(2\theta)}{2}\sqrt{1 + \sin(2\theta)}. \qquad (11)$$

For $\langle 100 \rangle$ oriented steps, i.e. $\theta = 45°$, the diffusivity becomes

$$\frac{b^2(\theta=45°)}{a_\perp^2} = \frac{1}{\sqrt{2}}\exp(-\epsilon_{\mathrm{NNN}}/k_B T). \qquad (12)$$

At $\theta = 45°$ the diffusivity due to forced kinks depends solely on the NNN interaction energy ϵ_{NNN}. In case $\epsilon_{\mathrm{NNN}} = 0$ (NN interactions only), the diffusivity is $b^2(45°)/a_\perp^2 = 1/\sqrt{2}$. For $\epsilon_{\mathrm{NNN}} < 0$ (repulsive NNN interactions) one has $b^2(45°)/a_\perp^2 > 1/\sqrt{2}$ and vice versa.

The important point is now that for a wide range of energies and temperatures the diffusivity is mainly determined by geometrically forced kinks. Thermal kinks contribute only for small angle θ. This is illustrated with Fig. 5. The figure compares the diffusivity $b^2(45°)/a_\perp^2$ due to geometrically forced kinks (dashed and dotted lines) to the exact solution [10, 13] for two cases: $\epsilon_{\mathrm{NN}} = 114\ \mathrm{meV}, \epsilon_{\mathrm{NNN}} = 28.5\ \mathrm{meV}$ and $\epsilon_{\mathrm{NN}} = 68\ \mathrm{meV}, \epsilon_{\mathrm{NNN}} = 6.8\ \mathrm{meV}$.

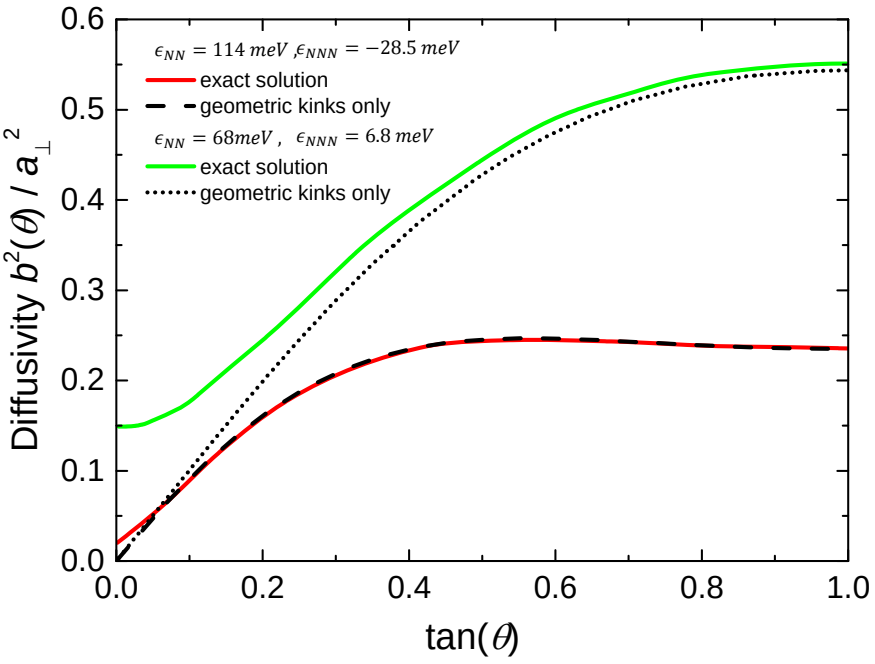

Fig. 5: The diffusivity $b^2(45°)/a_\perp^2$ due to geometrically forced kinks (dashed and dotted lines) is compared to the exact solution [10, 13] for two cases : $\epsilon_{\mathrm{NN}} = 114\ \mathrm{meV}, \epsilon_{\mathrm{NNN}} = 28.5\ \mathrm{meV}$ and $\epsilon_{\mathrm{NN}} = 68\ \mathrm{meV}, \epsilon_{\mathrm{NNN}} = 6.8\ \mathrm{meV}$. The temperature is 300K.

The temperature is set to 300K. Both cases assume specific sets with repulsive NNN interactions for which exact solutions have been published [10, 13]. For the case $\epsilon_{\mathrm{NN}} =$

$114\ \mathrm{meV}$, $\epsilon_{\mathrm{NNN}} = 28.5\ \mathrm{meV}$ ($\epsilon_{\mathrm{NNN}}/\epsilon_{\mathrm{NN}} = 1/4$), one finds a perfect agreement between the exact solution (red solid line) and the analytical equation for forced kinks only (dashed line) down to $\tan\theta = 0.05$. For $\epsilon_{\mathrm{NN}} = 68\ \mathrm{meV}, \epsilon_{\mathrm{NNN}} = 6.8\ \mathrm{meV}$ ($\epsilon_{\mathrm{NNN}}/\epsilon_{\mathrm{NN}} = 1/10$) one has larger deviation which tails off slowly with higher $\tan\theta$. Nevertheless, at $\theta = 45°$ the contribution of thermal kinks to the diffusivity is marginal.

Since the contribution of geometrically forced kinks vanishes at $\theta = 0°$ and thermal kinks play hardly a role at $\theta = 45°$, the two parameters ϵ_{NN} and ϵ_{NNN} can be determined from two experimental data points, the diffusivities at $\theta = 0°$ and $\theta = 45°$: Firstly, the NNN interaction energy ϵ_{NNN} is calculated analytically from $b^2(45°)/a_\perp^2$. The NN interaction energy ϵ_{NN} is then obtained by varying the value for ϵ_{NN} while keeping ϵ_{NNN} fixed until the diffusivity $b^2(0°)/a_\perp^2$ (eq. (7)) assumes the experimental value.

4. Line tension of $\langle 110 \rangle$ steps in the TSK model

The line tension of steps can be determined experimentally from equilibrium shape fluctuations of islands which are one atom layer high [25, 26] (see also Sect. 4.3.8 of [23]). Similar to the considerations of the diffusivity, a coarse-grained view on the surface is adopted, and the fluctuations are described employing statistical thermodynamics of fluctuations. The resulting line tension is therefore the free energy of steps in case of surfaces in vacuum and the equivalent to the free energy, now with the side condition of constant electrode potential instead of zero charge, in the case of electrode surfaces. The two energies deviate from each other except at the potential of zero charge [27, 28]. Since the quantity is obtained from the circumference of islands, the resulting line tension is a weighted average over all orientations. By invoking the inverse Wulff-construction on the equilibrium shape of islands of the same type, it is possible to obtain the line tension for

individual step orientations [29]. The method has been applied to islands on surfaces in vacuum [29, 30], as well as to islands on electrode surfaces [31]. In the context of this paper, the line tension of $\langle 110 \rangle$ steps is of particular interest. Experimental data as function of the electrode potential are available for three electrolytes [31-33] considered in part I. This section shows how the line tension of $\langle 110 \rangle$ steps can be expressed in terms of the NN and NNN interaction energies ϵ_{NN} and ϵ_{NNN}. The energetic part of the line tension in the TSK model follows immediately from eq. (5). The entropic term follows from the partition function *Z*. In our notation one therefore has for the line tension per atom

$$\beta_{\langle 110 \rangle} a_{||} = \epsilon_{\mathrm{NN}} + 2\epsilon_{\mathrm{NNN}} - k_{\mathrm{B}} T \, ln \, Z \tag{13}$$

The partition function contains contributions from all degrees of freedom. However, only the phonon degrees of freedom and the structural fluctuations (diffusivity) have sufficiently low energies to make a contribution to the free energy. The phonon part results from the difference in the phonon spectrum of stepped and flat surfaces. It has been calculated for steps on copper surfaces [34]. For $\langle 110 \rangle$ steps on Cu(100) surfaces, the vibrational contribution to the free energy at 300 K was found to be rather small (-2 meV/step atom). We therefore neglect the phonon contribution to the step free energy and focus on the structural part. The partition function due to step meandering is the denominator of eq. (3)

$$Z = 1 + 2 \sum_{n=1}^{\infty} e^{-\frac{\varepsilon_k(n)}{k_B T}}. \tag{14}$$

After inserting $\varepsilon_k(n)$ from eq. (4) one obtains

$$\beta_{\langle 110\rangle} a_{||} = \epsilon_{\mathrm{NN}} + 2\epsilon_{\mathrm{NNN}} - k_{\mathrm{B}}T \; ln\{1 + 2e^{2\epsilon_{\mathrm{NNN}}/k_B T}/(e^{(\epsilon_{\mathrm{NN}}+2\epsilon_{\mathrm{NNN}})/k_{\mathrm{B}}T} - 1)\} \quad (15)$$

We note that this equation is equivalent to eq. 4 in [14] derived in the context of the 2D Ising lattice. The entropic contribution to the free energy is of considerable magnitude when the energies involved in the kink generation are comparable to $k_{\mathrm{B}}T$, which is the case for surfaces in contact with an electrolyte; less so for surfaces in vacuum. Table 1 compiles samples of energy parameters obtained from step diffusivities in the TSK model with NNN interactions, ϵ_{NN} and ϵ_{NNN} for Au(100) in three different electrolytes and for Cu(100) in vacuum. The data for the different electrolytes refer to surface coverages between approximately 0.1-0.2 (SO_4^{2-}) and 0.2-0.5 (Br^-, Cl^-) anions per gold surface atom. The fifth column is the step energy per atom $E_{step} = \epsilon_{\mathrm{NN}} + 2\epsilon_{\mathrm{NNN}}$. The sixth column shows the entropic contribution TS_{step} to the step line tension. The last column compares the step line tension calculated in the TSK model with NNN interactions to experimental data (in brackets). The good agreement entails that the energy parameters obtained from the orientation dependence of step diffusivities describe the line tension obtained in independent experiments rather well. The NNN TSK model is therefore an adequate basis for the description of the energetics of steps, while the NN model fails completely in most cases. For gold in Cl^- and Br^- e.g., the step energy E_{step} and therefore also the step line tension would be calculated twice as high, if the repulsive interaction between NNNs were neglected. For Cu(100) in vacuum on the other hand, neglect of the attractive NNN interactions would result in a step energy of 129 meV per atom, only about half the actual value.

Surface	coverage	ϵ_{NN}/meV	ϵ_{NNN}/meV	E_{step}/meV	TS_{step}/meV	line tension/meV
Au(100)/SO_4^{2-}	0.17	54	2	58	7	51 (52)
Au(100)/Cl^-	0.43	62	-12	38	6	32 (27)
Au(100)/Br^-	0.4	71	-19	33	4	29 (27)
Cu(100)	-	129	40	209	0.35	209 (220)

Table 1: Energy parameters obtained from step diffusivities in the TSK model with NNN interactions ϵ_{NN} and ϵ_{NNN} for Au(100) in three different electrolytes and Cu(100) in vacuum. The fifth column is the step energy per atom, $E_{step} = \epsilon_{\mathrm{NN}} + 2\epsilon_{\mathrm{NNN}}$. The sixth column shows the entropic contribution TS_{step} to the step line tension. The final column compares the step line tensions calculated in the TSK model with experimental data obtained from island shape fluctuations (in brackets) [35, 36].

5. Conclusion

By mapping NN and NNN interaction energies ϵ_{NN} and ϵ_{NNN} onto the "corner model", the diffusivity of step in $\langle 110 \rangle$ direction is calculated in closed form. The diffusivity of steps oriented along the $\langle 100 \rangle$ direction is well described (up to the fourth order in $\exp[-(\epsilon_{\mathrm{NN}} + 2\epsilon_{\mathrm{NNN}})/k_{\mathrm{B}}T]$) by a simple equation, which involves only the NNN energy. Hence, the two energetic parameters of the NNN model can be calculated from the diffusivities of steps oriented along the $\langle 110 \rangle$ and $\langle 100 \rangle$ directions. The step line tension calculated in the TSK model with NNN interactions included agrees well with experimental data obtained in independent experiments.

Acknowledgements

The work profited from helpful discussion with T.L. Einstein, Univ. Maryland, College Park and from his critical and thorough reading of the manuscript. TJ and MG thank the financial support from the DFG (Deutsche Forschungsgemeinschaft). TJ additionally acknowledges

financial support from the European Research Council through the ERC-StartingGrant THEOFUN (Grant Agreement No. 259608).

References

[1] M. Giesen, D.M. Kolb, Surf. Sci., 468 (2000) 149.

[2] M. Giesen, Prog. Surf. Sci., 68 (2001) 1.

[3] M. Giesen, S. Baier, J. Phys.: Condens. Matter, 13 (2001) 5009.

[4] S. Baier, S. Dieluweit, M. Giesen, Surf. Sci., 502/503 (2002) 463.

[5] S. Dieluweit, M. Giesen, J. Phys.:Cond. Mat., 14 (2002) 4211.

[6] S. Dieluweit, H. Ibach, M. Giesen, Faraday Discussions., 121 (2002) 27.

[7] H. Ibach, M. Giesen, W. Schmickler, J. Electroanal. Chem., 544 (2003) 13.

[8] M. Giesen, Surf. Sci., 370 (1997) 55.

[9] M. Poensgen, J.F. Wolf, J. Frohn, M. Giesen, H. Ibach, Surf. Sci., 274 (1992) 430.

[10] T.J. Stasevich, T.L. Einstein, R.K.P. Zia, M. Giesen, H. Ibach, F. Szalma, Phys. Rev. B, 70 (2004) 245404.

[11] C. Rottman, M. Wortis, Phys. Rev., B 24 (1981) 6274.

[12] N. Akutsu, Y. Akutsu, Surf. Sci., 376 (1997) 92.

[13] T.J. Stasevich, T.L. Einstein, Multiscale Model. Simul., 6 (2007) 90.

[14] H.J.W. Zandvliet, Europhys. Lett., 73 (2006) 747.

[15] H.J.W. Zandvliet, H.J.W. Zandvliet, Europhys. Lett., 74 (2006) 1123.

[16] N. Akutsu, J. Phys. Soc. Jpn., 61 (1992) 477.

[17] Y. Akutsu, N. Akutsu, J. Phys A: Math. Gen., 19 (1986) 2813.

[18] W. Kossel, Nachr. Ges. Wiss. Göttingen, 135 (1927).

[19] N.C. Bartelt, T.L. Einstein, E.D. Williams, Surf. Sci., 240 (1990) L591.

[20] H.-C. Jeong, E.D. Williams, Surf. Sci. Rep., 34 (1999) 171.

[21] M. Giesen, Prog. Surf. Sci., 68 (2001) 1.

[22] B.S. Swartzentruber, Y.-W. Mo, R. Kariotis, M.G. Lagally, M.B. Webb, Phys. Rev. Lett., 65 (1990) 1913.

[23] H. Ibach, Physics of Surfaces and Interfaces, Springer, Berlin, Heidelberg, New York, 2006.

[24] N.C. Bartelt, T.L. Einstein, E.D. Williams, Surf. Sci., 276 (1992) 308.

[25] S.V. Khare, T.L. Einstein, Phys. Rev. B, 54 (1996) 11752.

[26] S.V. Khare, T.L. Einstein, Phys. Rev. B, 57 (1998) 4782.

[27] M. Giesen, G. Beltramo, J. Müller, H. Ibach, W. Schmickler, Surf. Sci., 595 (2005) 127.

[28] H. Ibach, W. Schmickler, Phys. Rev. Lett., 91 (2003) 016106.

[29] C. Steimer, M. Giesen, L. Verheij, H. Ibach, Phys. Rev. B, 64 (2001) 085416.

[30] C. Bombis, H. Ibach, Surf. Sci., 564 (2004) 201.

[31] M. Al-Shakran, L. Kibler, T. Jacob, G. Beltramo, M. Giesen, Electrochemica Acta, 180 (2015) 427.

[32] S. Dieluweit, M. Giesen, J. Electroanal. Chem., 524-525 (2002) 194.

[33] E. Pichardo-Pedrero, M. Giesen, Electrochim. Acta, 52 (2007) 5659.

[34] S. Durukanoğlu, A. Kara, T.S. Rahman, Phys. Rev. B, 67 (2003) 235405.

[35] E. Pichardo-Pedrero, M. Giesen, Electrochim. Acta, 52 (2007) 5659.

[36] S. Dieluweit, H. Ibach, M. Giesen, T.L. Einstein, Phys. Rev. B, 67 (2003) R 121410.